



Research Article

Finite Element Evaluation of Stress Distribution in the Buried Steel Pipelines in Presence of Polyethylene Coating

Soroosh Masoudnia¹, Pezhman Taghipour Birgani^{1,*}, Saeed Yaghoubi²

¹Department of Mechanical Engineering, Ahv.C., Islamic Azad University, Ahvaz, Iran

²Department of Mechanical Engineering, Faculty of Engineering, Ilam University, Ilam, Iran

*Corresponding author: Pz.Taghipour@iau.ac.ir

Article History:

Received:
12 July 2025
Revised:
20 August 2025
Accepted:
23 August 2025
Published in Issue:
31 December 2025

Abstract

Stress analysis of buried pipes is essential for safety, longer life, and prevention of structural failures. The present research work is related to the stress analysis in the gas transmission steel pipeline buried in the soil. The steel pipe has a three-layer polyethylene coating with viscoelastic properties. The stresses are caused by traffic loads, including the passage of vehicles on the surface, soil weight and fluid pressure inside the pipe. The stress analysis on the buried pipe for three different states including (I) static loading- pipe without coating, (II) static loading- pipe with viscoelastic coating, and (III) dynamic loading- pipe with viscoelastic coating have been performed using finite element method. The results of numerical modeling in ANSYS for static loading and uncoated pipe have been compared with the theoretical outcomes and the accuracy of the modeling has been confirmed. Based on the obtained observations, the dynamic loading and viscoelastic coating were able to affect the stress distribution created in the buried pipe, in comparison with the static loading without coating. Also, increasing the friction in the pipe-soil interface kept the tensile stress at the top of the pipe crown constant and had a negligible effect on the stress at the bottom of the crown.

Keywords: Stress analysis, Buried pipe, ANSYS, Viscoelastic coating, Finite element method

©2025 the Author(s). Published by the OICC Press under the terms of the [CC BY 4.0, Creative Commons Attribution License](https://creativecommons.org/licenses/by/4.0/), which permits use, distribution and reproduction in any medium, provided the original work is properly cited.

Cite this article: Masoudnia, S., Taghipour Birgani, P., Yaghoubi, S., (2025). Finite element evaluation of stress distribution in the buried steel pipelines in presence of polyethylene coating, *Journal of Solid Mechanics*, 17(04): Article 15. <https://doi.org/10.57647/Jsm.2025.1704.15>

1. Introduction

Today, the pipelines are employed to transfer the water and energy sources such as oil and gas [1]. Due to protection of the pipelines against the natural factors consisting of the corrosion, urban aesthetics and etc., these lines are carried out in the soil. Buried pipelines in the soil are affected by several parameters that should be considered in the design. These factors include the fluid pressure in the pipe, the changes in the temperature of the fluid, the weight of the soil, and the forces applied by the soil (such as vehicle movement and earthquake) [2-5]. These forces are taken

into account in the design of pipes that are on the road and train rails. In the designing pipelines that are off-road, some of these forces may be neglected. Investigating the stress distribution in composite structures is of particular importance [6, 7]. Due to the presence of the variable forces on the buried pipelines, checking the stress distribution is of particular importance [8-10]. Several studies have been conducted by researchers about the buried pipelines and their design. Watkins et al. [11] implemented a field test on polyethylene condenser pipes with variable diameters of 381 mm to 610 mm. The pipes were under the vehicle load and the height of the soil above

the pipe was 305 mm. The results of their study showed that the soil height was suitable for preventing vertical displacement exceeding the permissible limit. An experimental facility designed to evaluate the performance of small-diameter pipes was presented by Brachman et al. [12]. They reported the reduction of boundary friction to less than 5° and limiting the boundary deformation to less than 1 mm at a vertical surcharge of 1000 KPa supply an acceptable conditions for a buried pipe. Arockiasamy et al. [13] studied on the strength of high density polyethylene, PVC and metal pipes, under heavy vehicles loading in the highways. Their findings demonstrated that the vertical displacement limitation of the pipe is largely dependent on the pipe diameter and the position of the loading contact surface. In another study, Kang et al. [14] examined the short and long term behavior of buried corrugated polyethylene pipes using finite element method. They found that the force due to the soil weight on the crown of pipe was influenced by time, soil specification and contact conditions in soil-pipe interface. Goltabar and Shekarchi [15] experimentally and numerically researched on the influence of traffic load in the buried pipe. The buried pipes were made of steel and PVC. Their results indicated that the most stresses occur in the middle of the pipe. Zhou et al. [16] focused on local stress and mechanical deformation of the pipe in a long underground buried pipeline. They reported that increasing in the pipe thickness is an alternative solution. Zhang et al. [17] studied on the mechanical behavior of buried pipeline in overload condition. Their outcomes showed that increasing in internal pressure it first reduces and then enhances the stress and, consequently strain created in the pipe. The dynamic behaviors of a multi-span viscoelastic functionally graded material pipe has been researched via Deng et al. [18]. They found that this type of material exhibits some special dynamic behaviors of the pipe and it could significantly increase their stability compared to the aluminum and steel pipes. Jacques et al. [19] presented a guided wave system for corrosion monitoring in coated buried steel pipes. According to their outcomes, after 2 years of periodic data gathering, the collar demonstrated acceptable stability and it was able to identify corrosion defects found in the buried pipe. Wu et al. [20] investigated on stress and strain distribution in the buried PE pipelines. They reported that when the excavate angle was 30° or the excavation offset distance was $0.3D$, the critical load reached to the minimum value. A comprehensive study on mechanical behavior of buried PE pipe under land subsidence was performed by Wu et al. [21]. They succeeded in obtaining the quantitative relationship between the transition length and pipeline failure mode using nonlinear regression analysis. Peric et al. [22] investigated on residual stresses in buried-arc welded pipe.

The practical residual stress evaluations on the outside surfaces of the welded model were validated by simulation outcomes using the X-ray diffraction method. Khan et al. [23] focused on stress distribution around the conduit buried pipe, experimentally. They found that the crest distance of the conduit from the slope edge and the finding soil-conduit interaction, governed the stress distribution and its structural replication to applied fluid pressure. A study on dynamic behavior of buried pipeline considering the pipe connection form in presence of blasting seismic waves was done by Zhao et al. [24]. They reported the flange bolt joint is vulnerable to the adverse influence of blasting vibration and the safety evaluation of pipeline. Zhang et al. [25] investigated on mechanical response of buried pipeline under traffic load. They employ modified machine learning model to study the influences of several parameter such as diameter, wall thickness and buried depth on mechanical response obtained from buried pipelines. Wu et al. [26] studied on damage assessment of HDPE pipe subjected to blast loads. They presented new prediction model of pipe corresponded to different damage level. Their findings revealed that by decreasing the distance from the explosive, the peak particle velocity of pipe and surface enhances. In another study, Yang et al. [27] analyzed the PE pipeline under rockfall conditions. In their research, the effects of rockfall radius, pipe burial depth, and rockfall impact velocity on dynamic response of buried pipe have been investigated. Zhang and Wong [28] focused on the effects of corrosion on buried pipe under external load. According to their experimental and numerical outcomes, the simulated corrosion holes enhance the stress created in the buried pipe. Using of appropriate coatings is one of the most effective methods to prevent the corrosion of the external surfaces of gas transmission pipelines buried in the soil. In the present research work, the stresses distribution in gas transmission steel buried pipes with three-layer polyethylene coating, which has viscoelastic properties, have been analyzed. The stresses on the pipe for three different states of static loading-pipe without coating, static loading-pipe with viscoelastic coating, and dynamic loading-pipe with viscoelastic coating have been calculated using the finite element method. Based on the previous studies studied, it can be said that no comprehensive research has been done on stress distribution in buried steel pipe with three-layer polyethylene coating under various loading conditions.

2. Theoretical basis

The safety of buried pipes, as one of the most important urban and road facilities, under different loading conditions is highly dependent on the safe design and performance of these pipes [29].

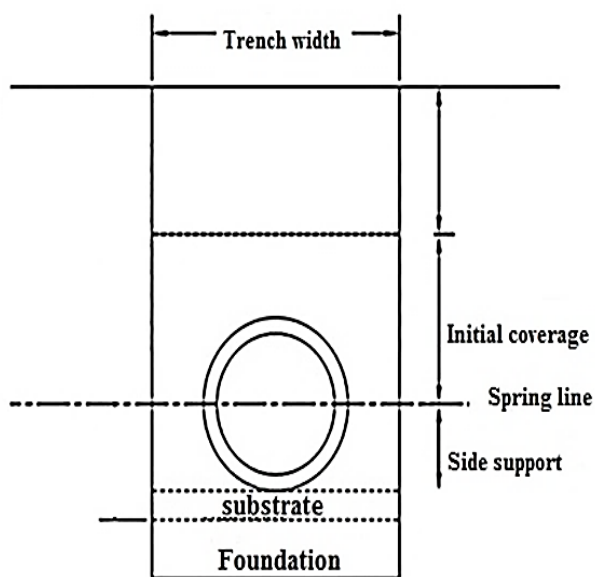


Figure 1. The schematic of pipe deployment in the trench

This important state can only be achieved by analyzing and understanding their real behavior and applying it in design. In general, bursting methods are carried out in the embankment and the trench.

Due to the fact that the implementation method for drainage, sewage, water supply and gas pipelines is mostly installed in the trench, this method has also been used for burglary. The schematic of pipe deployment in the trench is presented in Figure 1.

In this method, the pipe is placed in a trench dug into the unloaded soil and is immersed on it. The most important issue in installation of buried pipes is the interconnection of pipe-soil in relation to each other.

In fact, the pipe-soil system acts as a composite structure in which the properties of the system can be in addition to the average properties of the components.

2.1. Vertical pressure on the pipe crown

The force on the buried pipe is affected by the dead and overhead loads. The dead load is due to the weight of the soil and the pavement above the pipe. In other hand, the overhead loads are including the forces caused by vehicles and structures on the surface.

In the design of buried pipes, the maximum load applied to the pipe crown as the dead load is considered equal to the weight of the soil column above the pipe.

This load is often recognized as a prismatic force. This force is a simple method for calculating the pressure caused by the soil weight on the pipe.

The remarkable point is that the actual force applied to the pipe, due to the transfer of a portion of the shear strength to the walls of the soil around the pipe, is less than the

pressure force. This transfer of force will reduce the vertical pressure of the soil on the pipe [30].

2.1.1. Prismatic load

When the soil is homogeneous and does not contain empty spaces, the simple method to determine the vertical pressure on the crown of the pipe is using prismatic force. In this case, the force of prism is calculated from Eq. (1):

$$P_E = WH \tag{1}$$

where, P_E is the vertical pressure of the soil on the pipe crown, W is the specific gravity of the soil, and H is the height of the soil above the pipe crown [30].

2.1.2. Marston load

One of the methods for calculating the vertical pressure caused by soil column on the pipe crown is the Marston load method, which usually represents a more realistic value than the prismatic load.

According to a series of practical experiments, Marston et al. published the method of designing the buried pipe in 1930.

He assumed that the shear stress in the trench wall would reduce the pressure exerted on the pipe [31]. Therefore, Marston provides Eq. (2) for determining the pressure caused by the soil weight applied to the pipe:

$$P_M = C_D W B_D \tag{2}$$

where, P_M is the vertical pressure of the soil on the pipe crown, B_D is the width of the trench at the top of the pipe, and C_D is the force coefficient and is calculated as follows (Eq. (3)):

$$C_D = \frac{1 - e^{-2k\mu' \frac{H}{B_D}}}{2k\mu'} \tag{3}$$

In this equation, μ' is the coefficient of friction between the soil in the trench and the trench wall and k is the ground pressure coefficient and is expressed as Eq. (4):

$$k = \tan^2(45 - \frac{\phi}{2}) \tag{4}$$

where, ϕ is the internal friction angle of the soil. The $k\mu'$ values are expressed in Table 1 [30].

Table1. $k\mu'$ quantities for several soil samples [30]

Soil type	$k\mu'$
Saturated clay	0.11
Ordinary clay	0.13
Soil clay saturation	0.15
Sand	0.165
Grained and clean soils	0.192

2.1.3. Corrected prismatic force

The actual pressure exerted on the buried pipe is a combination of Marston and prism loads and is computed as follows (Eq. (5)):

$$P_C = P_M + 0.4(P_E - P_M) \Rightarrow P_C = 0.6P_M + 0.4P_E \quad (5)$$

In the above equation, P_C is the corrected prism load.

2.1.4. Pressure on the pipe caused by surface loads

Surface loads are usually considered as massive forces such as building foundations, and centralized forces such as car wheels.

The distribution of pressure in the soil reduces the effect of surface force by increasing the depth or the horizontal distance from the force level.

Also, the amount of pressure at the bottom of the surface force depends on the amount of surface force and the surface of its effect.

2.1.4.1. The vehicle force applied by the wheels

Based on the AASHTO standard, the Busink centralized force equation is defined as Eq. (6) for calculating the wheel force, regardless of the pavement effects [32]:

$$P_L = \frac{3IW_L H^3}{2\pi r^5} \quad (6-a)$$

$$r = \sqrt{X^2 + H^2} \quad (6-b)$$

where, I is the coefficient of collision, W_L is the wheel force, H is the depth of the buried pipe, and r represents the distance between the pipe crown and the point of force effect (Figure 2).

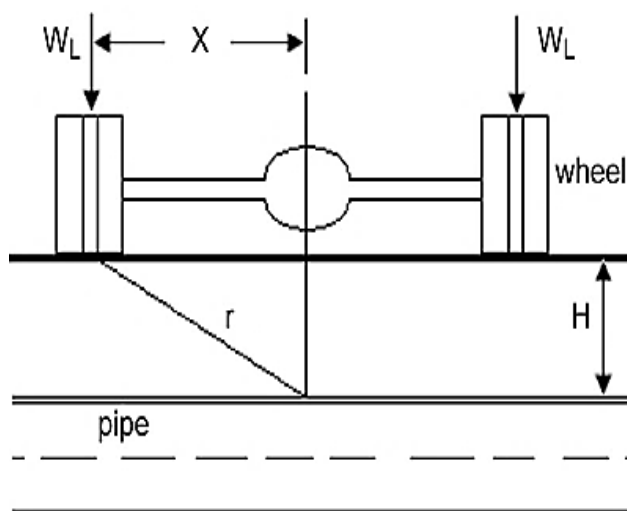


Figure 2. The effect of wheel force on the buried pipe [32]

2.2. Stress in buried steel pipes

Buried pipes are subjected to stress due to the combination of internal and external forces. In these pipes, the greatest force is corresponded to the gas pressure. For pressurized buried pipes, the internal pressure may be greater than the radial external pressure caused by the soil. As a result, the tensile stresses are created in the pipe wall. Therefore, the compressive stresses in the pressure pipes are negligible. When the pipe is under the uniform radial pressure caused by the soil column, the compressive stress in the wall of the pipe is obtained from the following equation (Eq. (7)) [32]:

$$\sigma_c = \frac{P_T D}{2h} \quad (7)$$

In above equation, P_T is the total vertical force enters to the pipe, D represents the outer diameter of the pipe, and h is the thickness of the pipe.

2.3. Viscoelastic materials behavior

One of the most important and effective methods to prevent corrosion of the external surfaces in the buried gas transmission pipelines in the soil is to employ the appropriate coatings. Using of polyethylene coatings with viscoelastic properties is one of the most widely applied methods to keep the corrosion of the gas transmission pipes surfaces [33]. Viscoelastic property refers to materials that have viscous and elastic properties, simultaneously and, like many materials, do not fully comply from Hooke's law. In these materials, the relationship between the stress and strain depends on the time, and by keeping the stress constant, the strain increases over the time, which is called creep phenomenon [34].

3. Finite element modeling

3.1. Steel pipe properties

In the current research work, two modeling modes are considered, in both cases, the pipe is made of steel. According to the API 5L, the steel grade for the first and second cases are selected to X-52 ad X-42, respectively. Considering that the permissible limit of corrosion is 3 mm, the thickness of the pipe for the first and second cases are equal to, in turn, 14.27 mm and 5.2 mm. The geometrical and mechanical properties of buried pipe are considered, based on ASME B 31.4 and ASME B 31.8 [35, 36].

3.2. Specification of the used soils around the pipe

The pipes that are installed in off-road ways do not have concrete protection and asphalt surface.

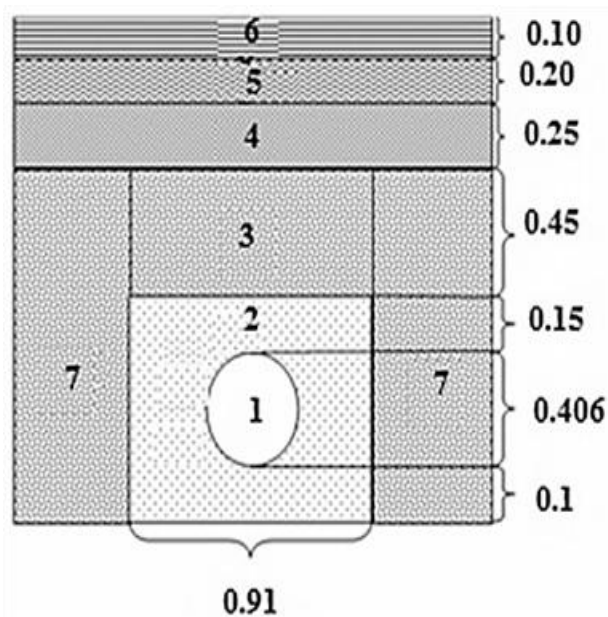


Figure 3. 2D schematic of the pipe installed in the trench (dimensions in meter)

Table 2. Standard thickness specification for steel pipes (dimensions in mm)

Pipe diameter	Epoxy powder resin (first layer)	Adhesion (second layer)	Total thickness
Up to nominal diameter 500	0.2	0.15	2.5

Therefore, in the modeling of soil layers, according to the description provided in the ASTM D2321 standard, the asphalt surface is removed. Figure 3 shows the layering of the soil in this state. Physical properties of soils used in the trench are considered based on Ref. [30].

3.3. The thickness of polyethylene coating

The thickness of the coating layers for the buried pipes follows certain rules. These rules are related to the material and dimensions of the pipe. Table 2 shows the specification of the standard coating thickness for steel pipes with a three layer polyethylene coating extracted from IPS-G-TP-335 [37].

As mentioned earlier, the polyethylene layer has viscoelastic properties.

Therefore, for viscoelastic models, the polyethylene modeling in software is employed. Among the methods presented, the Prony method is the most suitable manner for modeling the polyethylene materials. Prony series coefficients for polyethylene are expressed as a table. In this method, the shear modulus coefficients are used at the stress release times applied in the shear response section. The shear modulus G_i are extracted from Ref. [38] and fall into the $a_i = G_i/G_0$. The values of a_i obtained in the shear

response section applied in the corresponding time. In this study, the value of G_0 is considered to 369.3 MPa.

3.4. Simulation of the problem

After defining the material, the model geometry was created in the software. To apply symmetry conditions and reduce problem solving time, one half of the model was considered. The conditions between the soil layers are defined integrally, and the connection in soil-pipe common surface with contact conditions of the friction type and different friction coefficients were considered. The material of the modeled pipe is made of steel with viscoelastic coating.

According to this property, an element should be selected that has the capability of modeling for materials with viscoelastic properties. For this purpose, PLANE82 and SOLID186 elements have been employed. Considering that the soil is assumed to be elastic and the modulus of elasticity, Poisson's ratio and constant density are considered for it, the desired elements for soil modeling can be selected from among the structural elements of ANSYS. Accordingly, SOLID95 element has been used to model the soil in three-dimensional mode. In the finite element analysis, meshing is one of the most important steps. A view of the 2D- model with appropriate meshing is given in Figure 4.

In the next step, the existing loads, including the force caused by soil weight, internal pressure and traffic load, are applied to the model. Since the pipe is modeled for gas transferring, the internal pressure for the first case is 170 bar (2465 psi) and second case is considered to 4 bar (58 psi), which are equivalent to the pressure of the pumping station in Iran.

To apply the traffic load, according to the AASHTO standard, the force applied on two surfaces, each of which has an area of 18*20 in² and a distance between them of 72 in, is entered to the outer surface of the soil in the amount of 71174 N. Due to the mobility of the traffic load, this load is considered as a variable in time. In general, the traffic load has a recurring state, which indicates the changes of this load over time.

To establish the boundary and loading conditions, the problem solving time is divided into three intervals. In the first step, the gravitational acceleration is considered to apply the weight of the soil. In the second and third time periods, the pressure caused by the gas transfer and the vehicle's passing force on the soil surface have been taken into account.

On the bottom of the lowest layer of soil, a fixed constraint is included that restrains all the degrees of freedom in this region. Figure 5 shows the load and boundary conditions applied on the model.

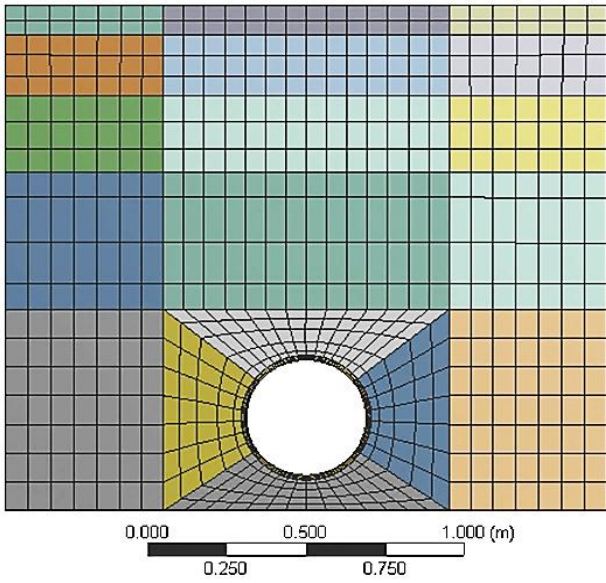


Figure 4. Two-dimensional view of the pipe mesh, coating and surrounding soil

A: Transient Structural
 Transient Structural (A5)
 Time: 32. s
 2/3/2018 12:24 AM

- A Fixed Support
- B Force: 71000 N
- C Pressure: 1.7e+007 Pa
- D Acceleration: 9.806 m/s²
- E Force 2: 71000 N

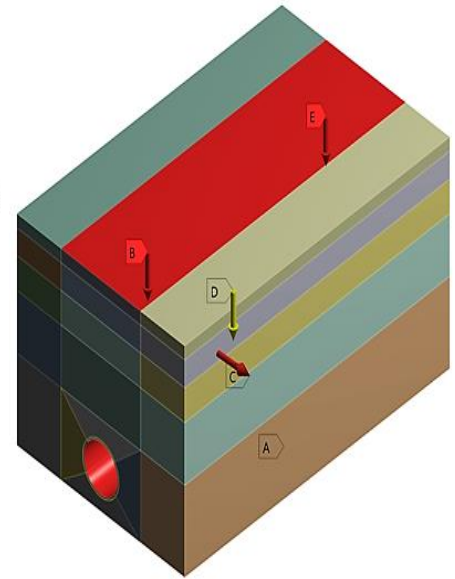
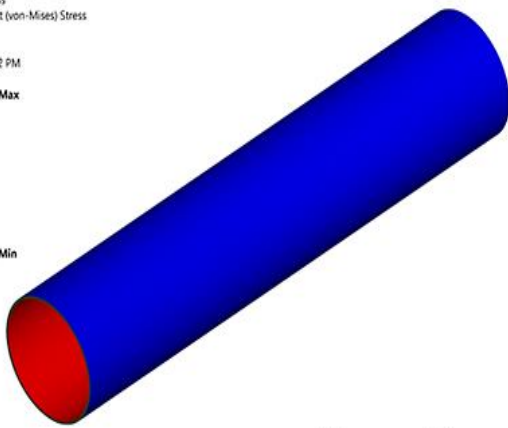


Figure 5. Loading and boundary conditions applied to the FE model

A: Transient Structural
 Equivalent Stress
 Type: Equivalent (von-Mises) Stress
 Unit: Pa
 Time: 32
 12/15/2017 7:12 PM

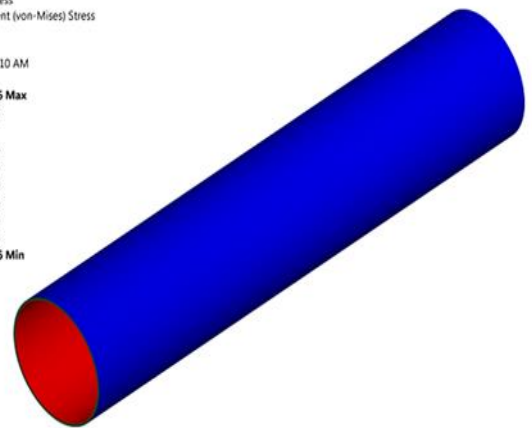
2.4846e8 Max
 2.4535e8
 2.4225e8
 2.3915e8
 2.3604e8
 2.3294e8
 2.2983e8
 2.2673e8
 2.2362e8
 2.2052e8 Min



(a)

A: Transient Structural
 Equivalent Stress
 Type: Equivalent (von-Mises) Stress
 Unit: Pa
 Time: 32
 12/29/2017 4:10 AM

5.8461e6 Max
 5.7731e6
 5.7e6
 5.6209e6
 5.539e6
 5.4808e6
 5.4078e6
 5.3347e6
 5.2617e6
 5.1886e6 Min



(b)

Figure 6. The von-Mises stress contours in (a) first mode and (b) second mode of buried pipe

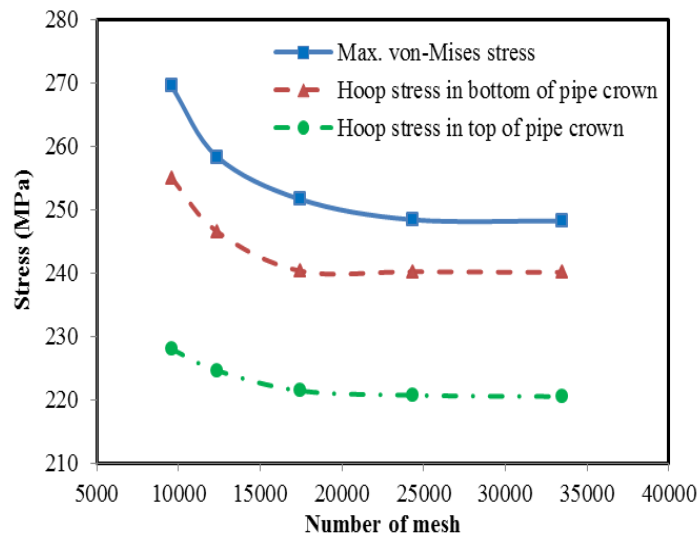


Figure 7. The convergence test results

4. Results and discussion

The von-Mises stress contours caused by soil weight, fluid pressure and traffic load for the first and second modes in buried pipe are shown in Figure 6. As it is clear, the maximum amount of von-Mises stress in the first and second modes are computed about 248.5 MPa and 5.8 MPa, respectively.

4.1. Convergence test

In the finite element analysis, the number of meshes can have a significant effect on the final solution. Therefore, this issue should be carefully investigated. The influences of the mesh number on the stress values for the first mode of the main model have been researched (Figure 7). According to the convergence test, the numbers of elements were considered to 33500.

4.2. Verification of the numerical results

In the current section, the aim is to check the accuracy of the numerical results obtained from the simulation of the model. For this purpose, the pipe has been modeled under the effect of the force caused by the weight of the soil and the vehicle, and the amount of stress in the pipe crown extracted from the finite element solution has been compared with the outcomes gained from the theoretical relationships (section 2). The values of forces caused by the soil and vehicle are presented in Table 3.

Table 3. Soil and vehicle load values

No.	Loading type	Value (Pa)
1	Prismatic load	20444.85
2	Marston load	16483.6759
3	Vehicle load	22568.7768
4	Corrected prismatic load	18068.1455
5	Soil & vehicle load	40626.9223

The summary of the theoretical and numerical findings obtained to calculate the amounts of stress in the buried pipe are given in Table 4. Based on the error values, it can be said that the simulation results have an acceptable accuracy.

4.3. The effect of changing the dimensions of the model

In the present section, the dimensions of the model that can be used to calculate stresses are determined according to the effect of soil weight, vehicle weight and the internal pressure of the buried pipe. For this purpose, the maximum values of von-Mises and hoop stresses are checked for the changing of soil dimensions in the lower and upper part of the pipe crown.

4.3.1. Changing the transverse dimension of the model

In the simulation of the buried pipe, by setting the its length and soil (z) equal to 3 m, the changes in the width of the soil (x) and its effects on the stress are discussed. The influences of soil transverse dimension change on the different stress are presented in Table 5. Based on the results, it can be concluded that by increasing in the transverse dimension of the model, the von-Mises and the hoop stresses are enhanced, regardless of its modes.

4.3.2. Changing the longitudinal dimension of the model

The purpose of this section is to investigate the influence of longitudinal dimension changes on the stresses created in the buried pipe. Therefore, the transverse dimension of the current model is equal to 1.91 m and its length is considered variables. In Table 6, the values of the stresses created in the pipe for changes in its length are given. The findings presented in Table 6 demonstrated that with the increase in the length of the model, the von-Mises stress increased, while the hoop stresses at the bottom and top of the pipe crown remain constant.

Table 4. Theoretical and FEM values of stresses

No.	Stress Type	Theoretical (MPa)	FEM (MPa)		First mode error	Second mode error
			Mode I	Mode II		
1	Stress caused by soil	0.257	0.276	0.248	7.39 %	5.7 %
2	Stress caused by soil & vehicle	0.579	0.625	0.612	7.94 %	3.5 %

Table 5. Stress variations in the buried pipe due to soil transverse dimension changes

Upper surface of the model (x*z)	Max. von-Mises stress (MPa)		Hoop stress at bottom of the pipe crown (MPa)		Hoop stress at top of the pipe crown (MPa)	
	Mode I	Mode II	Mode I	Mode II	Mode I	Mode II
1.91*3	248.42	5.72	239.29	5.61	220.71	5.19
2.91*3	251.35	5.81	242.15	5.75	223.36	5.22
3.91*3	252.24	5.93	242.91	5.91	224.18	5.28

Table 6. Stress variations in the buried pipe due to soil longitudinal dimension changes

Upper surface of the model (x*z)	Max. von-Mises stress (MPa)		Hoop stress at bottom of the pipe crown (MPa)		Hoop stress at top of the pipe crown (MPa)	
	Mode I	Mode II	Mode I	Mode II	Mode I	Mode II
1.91*3	248.46	5.81	239.28	5.63	220.69	5.19
1.91*4	248.94	5.90	239.29	5.63	220.71	5.20
1.91*5	249.26	5.98	239.29	5.63	220.71	5.19

Table 7. The effect of friction coefficient in soil-pipe contact surface on variation of stresses

Friction coefficient	Max. von-Mises stress (MPa)		Hoop stress at bottom of the pipe crown (MPa)		Hoop stress at top of the pipe crown (MPa)	
	Mode I	Mode II	Mode I	Mode II	Mode I	Mode II
0	248.17	5.84	239.11	5.63	220.43	5.19
0.1	249.46	5.88	239.18	5.64	222.12	5.32
0.5	251.20	6.06	239.55	5.67	223.91	5.39
1	253.49	6.22	239.84	5.71	224.78	5.64

Table 8. Stress values for different loading conditions

No.	Loading	Von- Mises stress (Mpa)		Explanation
		Mode I	Mode II	
1	Stress due to soil weight	0.28	0.25	Transient load with viscoelastic coating
2	Stress due to soil weight and fluid pressure	248.13	5.79	
3	Stress due to soil weight and fluid pressure and traffic load	248.47	5.85	Static load with viscoelastic coating
4	Stress due to soil weight	0.28	0.25	
5	Stress due to soil weight and fluid pressure	248.13	5.79	Static load without any coating
6	Stress due to soil weight and fluid pressure and traffic load	248.45	5.83	
7	Stress due to soil weight	0.28	0.25	Static load without any coating
8	Stress due to soil weight and fluid pressure	248.14	5.79	
9	Stress due to soil weight and traffic load	0.63	0.62	Static load without any coating
10	Stress due to soil weight and fluid pressure and traffic load	248.51	5.87	

4.4. Slipping effect in soil-pipe contact surface

In the current section, the effect of slipping in the soil-pipe contact surface on variation of stress created in the buried pipe has been investigated. Considering that one of the important parameters in contact conditions is the friction coefficient between two surfaces, in Table 7, the influence of slippage on the stresses in the pipe is shown. According to the position of the soil and the pipe, considering the sliding effect has negligible effect on the hoop stresses at the bottom of the pipe. Von-Mises stresses at the bottom of the pipe crown increase with the enhancing of the friction coefficient. In the present research, the friction coefficient between two mentioned surfaces is considered to be 0.1.

4.5. Stress for different loading

Each of the three forces mentioned in section 4.2 has a different effect on the buried pipe. The aim of present section is to examine these effects. For this purpose,

various combinations of loading on the pipe have been applied and the results obtained from them are summarized in Table 8. Based on the results, it can be stated that most of the stress created is due to the presence of fluid pressure inside the pipes. After the fluid pressure, the force caused by the traffic load has the greatest effect on the amount of stress created in the buried pipe. According to Table 8, it can be said that the effect of transient load increases the amount of stress and the influence of coating reduces it. In general, the stress has decreased by 0.3% in comparison with the static load state and without coating.

5. Conclusion

In the current research, the stress distribution due to fluid pressure, soil weight and traffic load in the buried pipe has been investigated. The used pipe is made of steel with three-layer polyethylene coating, which has viscoelastic properties. The numerical simulation of the problem has been done using ANSYS software. The stresses on the

pipe for three different states of (I) static loading- pipe without coating, (II) static loading- pipe with viscoelastic coating, and (III) dynamic loading- pipe with viscoelastic coating have been investigated. A summary of the research results are given below:

- The maximum stress in all load conditions occurs at the bottom of the pipe crown. This is due to the presence of a maximum of three forces, namely the weight of the soil, the fluid pressure and the vehicle.
- It was observed that the effect of transient load increases the amount of stress by about 0.4% and the effect of coating reduces it by about 0.7%. In general, the stress has decreased by 0.3% compared to the static load state and without coating.
- Increasing the transverse dimension of the model will increase the von-Mises stresses at the bottom of the pipe crown, where the most stresses enter the pipe, as well as the hoop stresses at the bottom and top of it. In the other hand, as the length of the model increases, the von-Mises stresses at the bottom of the pipe crown increases, but the hoop stresses at the bottom and top of the pipe crown remain constant.
- As the friction between the pipe and the soil increases, the tensile stress at the top of the pipe crown is almost constant and the tensile stress at the bottom of the pipe crown rarely increases whose its effects are small and negligible.

Authors Contribution

Soroosh Masoudnia: Software, Formal analysis, Data curation.
Pezhman Taghipour Birgani: Methodology, Investigation, Writing-Original draft, Resources.
Saeed Yaghoubi: Conceptualization, Project administration, Supervision, Writing- Original draft.
All authors reviewed the manuscript."

Availability of data and materials

The data that support the findings of this study are available from the corresponding author, upon reasonable request.

Conflict of interests

The author states that there is no conflict of interest.

References

- [1] Hussain, M., Zhang, T., Chaudhry, M., Jamil, I., Kausar, S., and Hussain, I. 2024. Review of prediction of stress corrosion cracking in gas pipelines using machine learning. *Machines* 12(1):42. <https://doi.org/10.3390/machines12>
- [2] Kennedy J. L. 1984. Oil and gas pipeline fundamentals. PennWell Publishing Company.
- [3] Datta, T. 1999. Seismic response of buried pipelines: a state-of-the-art review. *Nuclear engineering and design* 192(2-3):271-284.
- [4] Abdoun, T. H., Ha, D., O'Rourke, M. J., Symans, M. D., O'Rourke, T. D., Palmer, M. C., and Steward, H. E. 2009. Factors influencing the behavior of buried pipelines subjected to earthquake faulting. *Soil Dynamics and Earthquake Engineering* 29(3):415-427. <https://doi.org/10.1016/j.soildyn.2008.04.006>
- [5] Abubakar, A., Abisoye, O. A., Alabi, I. O., Solomon, A., and Oyefolahan, I. O. 2025. Systematic literature review and bibliometric analysis of pipeline monitoring and leakage detection techniques. *Discover Mechanical Engineering* 4(1):17. <https://doi.org/10.1007/s44245-025-00102-w>
- [6] Yaghoubi, S., and Shishesaz, M. 2023. A Novel Approach to Investigate Transient Stress Distribution Caused by Fiber Breakage in Simple and Hybrid Composite Materials. *Journal of Failure Analysis and Prevention* 23:325-338. <https://doi.org/10.1007/s11668-022-01584-6>
- [7] Shishesaz, M., Gatea, A. H., Moradi, S., and Yaghoubi, S. 2024. Stress analysis in the buried polyethylene pipes with viscoelastic behavior: a finite element study. *Discover Applied Sciences* 6(11):616. <https://doi.org/10.1007/s42452-024-06331-0>
- [8] Noor, M. A., and Dhar, A. S. 2003. Three-dimensional response of buried pipe under vehicle loads. *New Pipeline Technologies, Security, and Safety* 87:658-665. [https://doi.org/10.1061/40690\(2003\)87](https://doi.org/10.1061/40690(2003)87)
- [9] Zhang, Y., Hou, S., Lin, L., Lou, Y., and Zhou, Y. 2023. Experimental study on the mechanical behavior of buried steel pipeline subjected to the local subsidence. *International Journal of Pressure Vessels and Piping* 206:105037. <https://doi.org/10.1016/j.ijpvp.2023.105037>
- [10] Shishesaz, M., Yaghoubi, S., and Hussein, Gatea A. 2024. Numerical analysis of stress distribution in the pressurized composite pipe buried in the soil. *Journal of Adhesion Science and Technology* 38(20):3825-3841. <https://doi.org/10.1080/01694243.2024.2356917>
- [11] Watkins, R. K., Reeve, R. C., and Goddard, J. B. 1983. Effect of heavy loads on buried corrugated polyethylene pipe. *Transportation Research Record* 903:99-108.
- [12] Brachman, R. W., Moore, I., and Rowe, R. 2000. The design of a laboratory facility for evaluating the structural response of small-diameter buried pipes. *Canadian Geotechnical Journal* 37(2):281-295. <https://doi.org/10.1139/t99-104>
- [13] Arockiasamy, M., Chaallal, O., and Limpeteeprakarn, T. 2006. Full-scale field tests on flexible pipes under

- live load application. *Journal of performance of constructed facilities* 20(1):21-27.
[https://doi.org/10.1061/\(ASCE\)0887-3828\(2006\)20:1\(21\)](https://doi.org/10.1061/(ASCE)0887-3828(2006)20:1(21))
- [14] Kang, J. S., Han, T. H., Kang, Y. J., and Yoo, C. H. 2009. Short-term and long-term behaviors of buried corrugated high-density polyethylene (HDPE) pipes. *Composites Part B: Engineering* 40(5):404-412.
<https://doi.org/10.1016/j.compositesb.2009.01.006>
- [15] Goltabar, A. M., and Shekarchi, M. 2010. Investigation of traffic load on the buried pipeline by using of real scale experiment and Plaxis-3D software. *Research Journal of Applied Sciences, Engineering and Technology* 2(2):107-113.
- [16] Zhou, X., Yang, Z., and Han, P. 2015. Innovation design of long-distance pipelines buried under high-filling planned roads. *Natural Gas Industry B* 2(2-3):198-202.
<https://doi.org/10.1016/j.ngib.2015.07.011>
- [17] Zhang, J., Liang, Z., and Zhao, G. 2016. Mechanical behaviour analysis of a buried steel pipeline under ground overload. *Engineering Failure Analysis* 63:131-145.
<https://doi.org/10.1016/j.engfailanal.2016.02.008>
- [18] Deng, J., Liu, Y., Zhang, Z., and Liu, W. 2017. Dynamic behaviors of multi-span viscoelastic functionally graded material pipe conveying fluid. *Proceedings of the Institution of Mechanical Engineers, Part C: Journal of Mechanical Engineering Science* 231(17):3181-3192.
<https://doi.org/10.1177/0954406216642483>
- [19] Jacques, R. C., de Oliveira, H. H., dos Santos, R. W., and Clarke, T. G. 2019. Design and in situ validation of a guided wave system for corrosion monitoring in coated buried steel pipes. *Journal of Nondestructive Evaluation* 38:1-12.
<https://doi.org/10.1007/s10921-019-0604-7>
- [20] Wu, K., Zhang, H., Liu, X., Bolati, D., Liu, G., Chen, P., and Zhao, Y. 2019. Stress and strain analysis of buried PE pipelines subjected to mechanical excavation. *Engineering Failure Analysis* 106:104171.
<https://doi.org/10.1016/j.engfailanal.2019.104171>
- [21] Wu, Y., You, X., Zha, S. 2020. Mechanical behavior analysis of buried polyethylene pipe under land subsidence. *Engineering Failure Analysis* 108:104351.
<https://doi.org/10.1016/j.engfailanal.2019.104351>
- [22] Perić, M., Garašić, I., Gubelj, N., Tonković, Z., Nižetić, S., and Osman, K. 2022. Numerical Simulation and Experimental Measurement of Residual Stresses in a Thick-Walled Buried-Arc Welded Pipe Structure. *Metals* 12(7):1102.
<https://doi.org/10.3390/met12071102>
- [23] Khan, M. U. A., Shukla, S. K., and Paraskeva, T. S. 2022. Stress distribution around the conduit buried within a soil slope—An experimental investigation. *Transportation Geotechnics* 32:100687.
<https://doi.org/10.1016/j.trgeo.2021.100687>
- [24] Zhao, K., Jiang, N., Zhou, C., Li, H., Cai, Z., and Zhu, B. 2022. Dynamic behavior and failure of buried gas pipeline considering the pipe connection form subjected to blasting seismic waves. *Thin-Walled Structures* 170:108495.
<https://doi.org/10.1016/j.tws.2021.108495>
- [25] Zhang, D., Liu, X., Yang, Y., Shi, N., Jiang, J., Chen, P., Wu, X., Gao, H., and Zhang, H. 2022. Field experiment and numerical investigation on the mechanical response of buried pipeline under traffic load. *Engineering Failure Analysis* 142:106734.
<https://doi.org/10.1016/j.engfailanal.2022.106734>
- [26] Wu, T., Jiang, N., Zhou, C., Luo, X., Li, H., and Zhang, Y. 2022. Experimental and numerical investigations on damage assessment of high-density polyethylene pipe subjected to blast loads. *Engineering Failure Analysis* 131:105856.
<https://doi.org/10.1016/j.engfailanal.2021.105856>
- [27] Yang, Y. J., Liu, G. H., Yu, P., Huang, C., and Li, L. 2023. Dynamic response and safety analysis of polyethylene pipeline under rockfall conditions. *Quality and Reliability Engineering International* 39(5):2044-2068.
<https://doi.org/10.1002/qre.3383>
- [28] Zhang, Y., and Wong, R. C. K. 2023. Effect of corrosion on buried pipe responses under external load: Experimental and numerical study. *Tunnelling and Underground Space Technology* 132:104934.
<https://doi.org/10.1016/j.tust.2022.104934>
- [29] He, T., Gan, L., Liao, K., Liao, D., Xia, G., Chen, L., Gan, Y., Liao, J., and Tang, X. 2024. Quantitative study on dynamic response of buried natural gas pipeline under vehicle load. *Engineering Failure Analysis* 162:108454.
<https://doi.org/10.1016/j.engfailanal.2024.108454>
- [30] Moser, A. P., and Folkman, S. 2008. Buried pipe design. McGraw-Hill Education.
- [31] Marston, A. 1930. The theory of external loads on closed conduits in the light of the latest experiments. Highway research board proceedings.
- [32] Minervino, C., Sivakumar, B., Moses, F., Mertz, D., and Edberg, W. 2004. New AASHTO guide manual for

- load and resistance factor rating of highway bridges. *Journal of Bridge Engineering* 9(1):43-54. [https://doi.org/10.1061/\(ASCE\)1084-0702\(2004\)9:1\(43\)](https://doi.org/10.1061/(ASCE)1084-0702(2004)9:1(43))
- [33] Lakes, R. S. 2009. Viscoelastic materials. Cambridge university press.
- [34] Ferry, J. D. 1980. Viscoelastic properties of polymers. John Wiley & Sons.
- [35] Institute ANS. 1995. Gas transmission and distribution piping systems. American Society of Mechanical Engineers.
- [36] American National Standards Institute. Committee B31 CfPP. 2002. Pipeline Transportation Systems for Liquid Hydrocarbons and Other Liquids: ASME Code for Pressure Piping, B31. American Society of Mechanical Engineers.
- [37] Vazouras, P., Karamanos, S. A., and Dakoulas, P. 2012. Mechanical behavior of buried steel pipes crossing active strike-slip faults. *Soil Dynamics and Earthquake Engineering* 41:164-180. <https://doi.org/10.1016/j.soildyn.2012.05.012>
- [38] Hengprathanee, S. 2000. Evaluation of the geometry effect of the profile of high density polyethylene pipes. Ohio University.